Available online at www.sciencedirect.com

ScienceDirect

Procedia CIRP 62 (2017) 275 – 280

www.elsevier.com/locate/procedia

10th CIRP Conference on Intelligent Computation in Manufacturing Engineering - CIRP ICME '16

Statistical analysis and modelling of an Yb:KGW femtosecond laser micro-drilling process

Giuseppe Casalino[a,*], Aurora Maria Losacco[b], Angela Arnesano[b], Francesco Facchini[a], Maurizio Pierangeli[a], Cesare Bonserio[b]

[a]*DMMM, Politecnico di Bari, Viale Japigia 182, Bari 70124, Italy*
[b]*Laserinn, Strada Provinciale Casamassima km 3, Valenzano70010, Italy*

* Corresponding author. Tel.: +39-080-5962753; fax: 39-080-5962788. *E-mail address:* Giuseppe.casalino@poliba.it

Abstract

Femtosecond laser drilling is capable of economically drilling a number of closely located holes on micro-scale. Different characteristics or acceptance criteria like geometric and metallurgical factors are used to judge the quality of the drilled holes. This paper aims to evaluate the quality of micro-holes, which were drilled by Yb:KGW laser end-pumped by high-power diode bars. The geometric factors included hole roundness, hole taper and variation in hole entrance diameter. The metallurgical factors included recast layer and micro-cracks. The process parameters that most affected the hole quality were identified by the analysis of a full factorial design. Optimum hole characteristics on stainless steel sheet were studied by the ANOVA analysis. ANN model provided better insight into the best conditions for process adjustment, making possible simultaneous optimization of multiple responses.

Peer-review under responsibility of the scientific committee of the 10th CIRP Conference on Intelligent Computation in Manufacturing Engineering

Keywords: micro-drilling; Yb:kgw Laser; ANOVA; ANN.

1. INTRODUCTION

Nomenclature

YB:KGB	Ytterbium-Doped Potassium Gadolinium Tungstate
MZC	Minimum Zone Circle
IAD	Inlet Average Diameter
OAD	Outlet Average Diameter
T	Taper
D	Inlet nominal diameter
d	Outlet nominal diameter
fs	femtosecond

Laser processing of materials has proved to be an important tool for the development of micro-feature like micro-channel and micro-hole [1, 4]. Foil micro-drilling is suitable for numerous tasks and applications, electronic circuitry, optical surfaces, apertures and mechanical filters are just a few that can be mentioned [5].

Nanosecond lasers have been used for laser-machined through-holes. Nevertheless, compared to characteristic durations of laser radiation interaction with metals, nanosecond pulses are too long. The material is heated comparatively slowly, energy has a lot of time to diffuse into the surrounding area before the affected spot is heated enough for the material removal, which produces a large heat affected zone.

Moreover, the produced plasma plume interacts with the surface and brings about mostly negative consequences. Higher precision and better quality beyond the limits of a commercialized nanosecond pulsed laser system have been achieved using a cover plate [6].

Picosecond lasers offer high power for industrial scale fabrication and their pulse length adapt for metal fabrication because the characteristic durations of lattice heating are in the region of several to several tens of picoseconds [7].

Femtosecond lasers do not yet rival picosecond systems in delivered power, but with their parameters and industrial

Peer-review under responsibility of the scientific committee of the 10th CIRP Conference on Intelligent Computation in Manufacturing Engineering
doi:10.1016/j.procir.2016.06.111

robustness improving steadily, they seem destined to reach maturity in industry in the very near future. In fact, the technical advances in femtosecond laser technology are making laser machining of thin metallic coatings or foils a feasible solution for high-quality, deep drilling.

Femtosecond laser pulses provide a micromachining tool with high-quality material processing and large area patterning of solids. At relatively low laser fluence, i.e. close to the ablation threshold visible thermal or mechanical damage can happen [8].

For the smallest features and the least amount of heating and collateral damage, pulse lengths of femtosecond are almost as efficient as their picosecond alternative, and lead to the same morphologies inside the hole [9].

A study for aero-components like turbine airfoil indicated a complete absence of any melting, recast layers, heat-affected zones or microcracks close to the femtosecond laser micromachining of single crystal superalloys [10].

In fact, laser drilling has become the accepted economical process for drilling thousands of closely space holes in structures such as aircraft wings and engine components [11].

Femtosecond laser (fs) pulse provides the modification of surface or bulk of a transparent material with micrometer precision. A tightly one can deposit energy into a transparent material through high-order nonlinear absorption, producing 3D-localized material ablation either on the surface or in the bulk [12].

In micro-hole drilling and cutting using fs fiber laser (1030 nm wavelength and 750-fs pulse duration), no crack or collateral thermal damage was observed for both hard and soft tissue [13]. Even if femtosecond laser material processing at high laser fluences has provided a practical tool for high quality, deep drilling of metals, explanations supporting advantages of femtosecond lasers have to be given yet. Moreover, femtosecond lasers should be able to drill smaller holes than it is possible with other conventional techniques like wire EDM, punching, broaching, and to do this job with the same speed or faster [14].

Commercially available femtosecond laser sources, like Ti:sapphire based systems, allow to drill high quality holes but, unfortunately, the processing speed is still too low for many industrial applications. This disadvantage can be overcome by the new regenerative amplified solid state laser sources, providing much higher average powers and repetition rates. [15]. At this point, the full power of the ultrafast ytterbium-doped fiber CPA system achieves high quality holes, even without shielding gas [16].

Also double pulsed has been applied to bimetal micro-drilling and has been proven to be a good tool in controlling the ablation process [17].

Some parameters like the pulse duration of the applied laser source influence, the micro-drilling process of metals [18]. Therefore, the quality of a drilled hole in laser drilling depends on the right choice of the process parameters. Entry and exit circularity and taper are very important attributes which influence the drill quality [19].

The design of experiments (DOE) is adequate to study several process factors and their interactions complexity in order to solve problems by means of statistical analysis [20]. Multi-objective optimization of hole characteristics during pulsed Nd:YAG laser microdrilling of gamma-titanium aluminide alloy sheet was performed using both a central composite design (CCD) and response surface methodology (RSM) [19]. Precise modeling of stainless steel Nd:YAG laser percussion drilling was achieved by generalized neural network regression. This method permitted to adjust input parameters of the process in multipurpose and single purpose optimization modes [22].

Grey relational optimization approach combined with fuzzy methodology determined the optimum process parameters, which minimizes HAZ and hole circularity and maximizes material removal rate in a Pulsed Nd:YAG laser micro-drilling in high carbon steel within existing resources [23].

As reported in main theoretical and experimental studies in the literature [24], the removal of material by means of ultrashort laser pulses (ps, fs) substantially occurs through different mechanisms than ms and ns regimes laser processes since the thermal contribution is extremely reduced due to the pulse duration less than the time of electron-photon relaxation (0.5 ÷ 50 ps).

Fluence below 10 J/ cm^2 and "gentle ablation" regime produces high-precision micro machining using femtosecond laser pulses. In fact, higher fluences, i.e. under a "strong ablation" regime, induce alterations and irregularities, which compromise the quality of the hole with results comparable to those obtained by means of nanosecond lasers.

In this paper, the design of experiment and the artificial neural networks were used to create a statistical model for fs laser metal foil micro drilling. Tests were carried out on stainless steel 303 sheets with 0.17 mm thickness using a Yb:KGW femtosecond laser. A micro-hole array of 81 holes was drilled with 27 combinations of laser parameters, which were the pulse frequency, the pulse width, and the laser power.

The quality of the drilled holes was assessed by means of the analysis of the variance of inlet and outlet average diameters (IAD and OAD) and taper (T).

The recast layer and micro-crack were detected and analyzed by optical and scanning electron microscopy (Nikon Microscope and ZEISS EVO 40 XVP SEM).

Neural networks aimed to mapping the process parameters and hole features using Levenberg–Marquardt optimization [25, 26]. ANN took as input the statistical significant process parameters, which warranted a better converging and error performance.

2. Experimental set-up and procedure

The experimental set-up, as reported in Fig. 1, makes use of a Yb:KGW femtosecond laser PHAROS, λ= 1.03 µm with repetition rate in the range 1 KHz – 600 KHz single shot, and a pulse duration in the range 300 fs – 10 ps.

The system can work in linear mode by using of 3 linear axes and 2 rotational axes (Aerotech, work area 1000mmx1000 mm), or in scanning mode by using of a galvo scan head (Hurryscan, work area 7mmx7mm) and a beam shifting unit (WOP).

This configuration allows high accuracy machining (micro-cuts, micro-holes, micro-3D structuring, micro-markings etc.)

in industry and science field, in terms of dimensional accuracy, presence of defects and/or alterations induced in the material as a result of interaction with the laser radiation, process times.

Critical issues that satisfies:

• Micrometer dimensional tolerances

• Minimization of the alterations induced by the laser and thermal defects (cracks, burrs, oxidation)

• Ability to control the geometric parameters (hole taper, cut depth, inclination of the cutting edges)

• Significant variation of the effects of laser-matter as a function of the wavelength of the radiation and / or of the temporal width of the pulses.

• Minimization of process times.

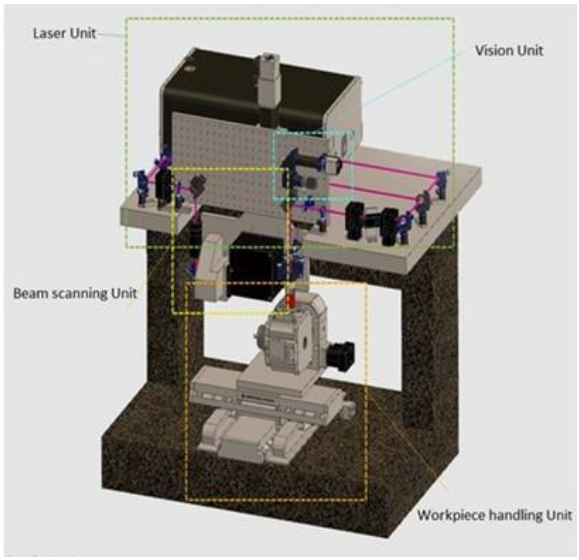

Fig. 1. Experimental device.

Micromachining was carried out in air using the laser operating at a repetition rate of 50 - 100 - 150 kHz and delivering individual pulses of 220 –-500 - 1000 fs duration, at three different average power of 4.5 - 5 - 5.5 W, by using the Beam Scanning Unit. Each experiment was repeated three times for a total of 81 micro holes. Table 1 contains the levels for each treatment. The sample was 0.17 mm thick stainless steel foil (steel grade - SAE 303).

Table 1. Factors and levels for each treatment.

Factors	Level 1	Level 2	Level 3
A: Pulse frequency (Hz)	50	100	150
B. Pulse width (fsec)	220	500	1000
C: Laser power (W)	4.5	5	4.5

Figure 2 shows the simplified geometrical features of the micro hole.

The roundness was evaluated with the Minimum Zone Circle (MZC) method. In this method, two circles are used as reference for measuring the roundness error. One circle is drawn outside the roundness profile just as to enclose the whole of it and the other circle is drawn inside the roundness profile so that it is just inscribed in the profile.

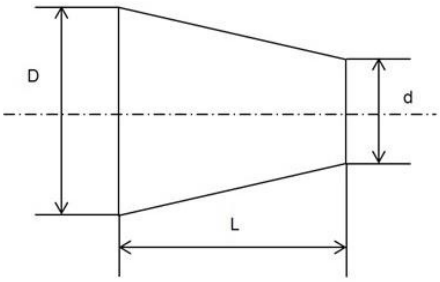

Fig. 2. Micro-hole geometric features.

The roundness error here is the difference between the radius of the two circles (see figure 3).

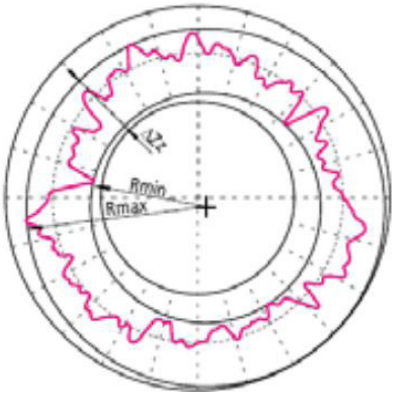

Fig. 3. Micro-hole roundness.

The inlet average diameter (IAD) and outlet average diameter (OAD) were calculated by the mean of the radius of the two circles for the inlet (D) and the outlet (d) diameters.

The taper (T) was calculated by the ratio of the difference between the inlet and outlet diameters of the sections to the foil thickness:

$$T = \frac{(D-d)}{L} \quad (1)$$

3. Analysis of variance

The adequacy of the developed mathematical models for the geometrical features of the micro-drilled hole generated by the Yb:KGW femtosecond laser was evaluated by the analysis of balanced variance.

Tables from 2 to 4 show the results in terms of F-ratio test and P-value. Lower than 0.05 p-values prove the significance of the factor on the response.

According to the tables of variance, the pulse frequency is significant for T and IAD and the pulse width is significant only for IAD and OAD. The interaction between the pulse frequency and pulse width is significant for T, IAD, and OAD.

Table 2. ANOVA table of results for taper (T).

Sources	DF	F	P-value
A	2	4.52	0.015
B	2	0.12	0.888
C	2	0.94	0.398
AB	4	10.73	0.000
BC	4	1.00	0.418
AC	4	1.29	0.284
ABC	8	0.43	0.899
Error	54		
Total	80		

Table 3. ANOVA table of results for inlet average diameter (IAD).

Sources	DF	F	P-value
A	2	9.47	0.000
B	2	18.16	0.000
C	2	0.75	0.639
AB	4	27.95	0.000
BC	4	1.21	0.931
AC	4	0.02	0.277
ABC	8	0.96	0.687
Error	54		
Total	80		

Table 4. ANOVA table of results for outlet average diameter (OAD).

Sources	DF	F	P-value
A	2	1,25	0,295
B	2	22,22	0,000
C	2	0,23	0,796
AB	4	4,40	0,004
BC	4	1,67	0,170
AC	4	0,41	0,802
ABC	8	0,82	0,590
Error	54		
Total	80		

4. Artificial Neural Network model

Approximate experimental models of the process have been developed by the generalized regression neural network tool (GRNN).

A Relationship between hole features and process parameters was established under different conditions. For this scope, the approach was based on the adoption of three different and independent networks. Consistently each ANN was used in order to predict only one of geometrical parameters.

A subset as big as 68% of the available experimental data, which was composed by 81 inputs/targets pairs, was used for the ANN training. In this phase, the synaptic weights, which are the links between neurons, has a synaptic weight attached. They were updated repeatedly in order to reduce the error between the experimental outputs and the associated targets.

A subset of 16% from the same experimental sample was adopted for validation. This phase consisting of identifying the underlying trend of the training data subset, avoiding the overfitting phenomenon.

The training process was stopped when the error began to increase. In order to deal with the overfitting problem, the training phase was stopped when the mean square error (MSE) assumed values lower than 0.01. The remaining data of the same experimental sample (16%) was been used for testing the forecast reliability of the ANN in the learning phase.

A random strategy was adopted for assigning the inputs/targets pairs to each subset.

4.1. ANN training and validation

The design of the ANN architecture consists in identifying the number of hidden layers and the number of neurons for each layer.

On one hand, many neurons can lead to memorize the training sets with and lost of the ANN's capability to generalise. On the other hand, a lack of neurons can inhibit appropriate pattern classification. In this work, a number of tests was performed varying the number of hidden layers and the number of neurons in the hidden layer.

In each case the best accuracy was achieved adopting an ANN architecture with two hidden layers. The number of input nodes, hidden (for each layer), and output nodes for every network are given in tables 5 thorough 7 at the line labelled "architecture".

Levenberg–Marquardt optimization was adopted to training the ANNs. Networks 1 and 3 were trained using the back propagation algorithm. This method allows to minimize the squares of the differences (E) between the desirable output, identified as $y_d(t)$, and the predicted output $y_p(t)$. 'E' is given by the follow equation:

$$E = \frac{1}{2} \sum_{t=1} \left(y_p(t) - y_d(t) \right)^2 \quad (2)$$

Levenberg–Marquardt algorithm was also adopted, which blends the 'Steepest Descent' method and the 'Gauss–Newton', therefore it can converge well even if the error surface is much more complex than the quadratic situation; ensuring, in many cases, speed and stability.

Levenberg–Marquardt algorithm can be presented as:

$$w_{k+1} = w_k - \left(J_k^T J_k + \mu I \right)^{-1} J_k e_k \quad (3)$$

Where J is Jacobian matrix, μ is the 'combination coefficient' (always positive), I is the identity matrix, and e represents the error vector. When μ is very small (nearly zero), Gauss–Newton algorithm is used. On the other hand, when μ is very large, steepest descent method is used.

In order to evaluate the reliability of the geometric parameters predicted by modelling, the features of the weld computed by ANN were compared to the experimental ones. For this scope, the Mean Absolute Percentage Error (MAPE) see equation 4, was calculated.

$$MAPE = \frac{1}{n} \sum_{i=1}^{n} \frac{x_i - \bar{x}_i}{x_i} \quad (4)$$

Back-propagation routine was trained with the steepest descent algorithm (eq. 3), where $\Delta w(k)$ is the vector of weights, $g(k)$ is the current gradient, $\alpha(k)$ is the learning rate, and m is the momentum parameter, which prevents that the algorithm converges to a local minimum or to a saddle point. Moreover, it avoids the risk of minimum overshooting, which can cause instability of the network. The learning rate and the momentum parameter are arbitrarily set to 0.01 and 0.99, respectively.

The training of the network was stopped when the mean square error (MSE) assumed values lower than 0.01.

4.2. ANN results and discussion

Tables 5 through 7 display the results of training and validation for the taper, the average inlet diameter, and the average outlet diameter, respectively.

Table 5. ANN table of results for taper (T).

	Sim-1	Sim-2	Sim-3	Sim-4
Input	A, B, C	A, A*B	A, A*B	A, A*B
Architecture	3-9-3-1	2-10-1	2-10-1	2-10-1
MAPE	9,55%	6,52%	9,55%	5,57%
n°iterations	50.424	50.000	37.000	72000

Table 6. ANN table of results for inlet average diameter (IAD).

	Sim-1	Sim-2	Sim-3	Sim-4
Input	A, B, C	A, B, A*B	A, B, A*B	A, B, A*B
Architecture	3-9-12-1	3-9-12-1	3-9-12-1	3-9-12-1
MAPE	6,35%	5,77%	6,35%	5,77%
n°iterations	50.754	50.000	28.700	49600

Table 7. ANN table of results for inlet average diameter (OAD).

	Sim-1	Sim-2	Sim-3	Sim-4
Input	A, B, C	B, A*B	B, A*B	B, A*B
Architecture	3-9-12-1	2-4-7-1	2-4-7-1	2-4-7-1
MAPE	8,00%	7,89%	8,00%	5,38%
n°iterations	50.214	50.000	42.000	78000

Sim-1 was performed regardless to the results of the ANOVA analysis. The pulse frequency, pulse width and taper were the input. Otherwise for Sim-2, Sim-3, and Sim-4, the input were the significant parameters accordingly to ANOVA results. They changed from one simulation to another. The reason was to assess the effects of statistically significant parameters on the network performance.

In particular, Sim-2 was stopped at 50000 iterations and MAPE was compared with that of Sim-1. It was found that Sim-2 network, which took into account the ANOVA results, had a lower MAPE with respect to that of the networks trained before the ANOVA.

Moreover, Sim-3 were stopped at the same MAPE of Sim-1. Again, after ANOVA networks had a better performance in terms of number of iterations that were required for a certain MAPE.

Eventually, Sim-4s were trained to their ultimate MAPE. It was found that their MAPEs were systematically lower than those of Sim-1.

5. Recast layer, spatters, and micro-crack

Recast layers, spatters, and microcracks commonly accompany laser-drilled holes. The overall quality of laser-drilled holes can be affected by those defects.

The high temperature on the work piece surface can cause thermal damage in the edge zones which has, as a rule, a negative influence on the components life. This condition is termed “the Recast Layer” [27].

Figure 4 shows the macrograph of a 10-hole array.

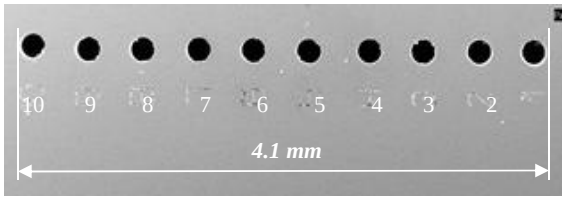

Fig. 4. Hole array outlook.

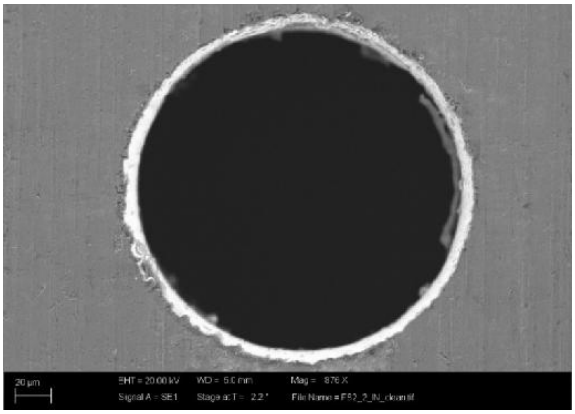

Fig. 5. Hole entrance, hole 8.

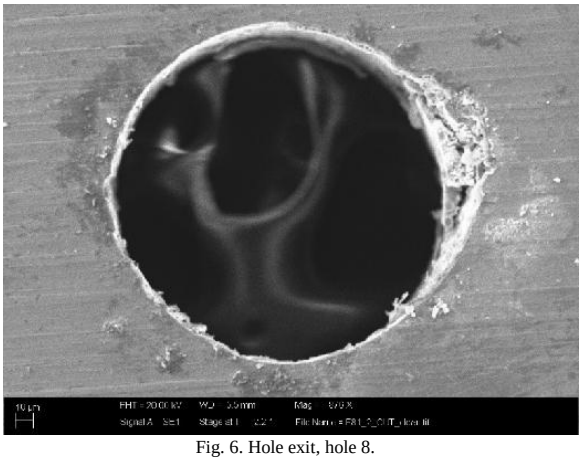

Fig. 6. Hole exit, hole 8.

In some holes, both entrance and exit surfaces were encircled by a thin irregular area, which represented the re-solidified layer. Either spattering deposits were absent or negligible (figs 5 and 6).

For some other holes, neither spatters nor recast layers were detected on the border of the hole drilled.

No cracks formed on the edge of any drilled micro-hole.

Eventually, the results pointed out that the lower level setting for pulse duration, pulse energy and laser wavelength would lead to enormous improvements in the quality of the hole, especially in respect of reduced recast layers and spatters.

6. Conclusions

Micro-holes, which were drilled by Yb:KGW laser end-pumped by high-power diode bars showed very thin or absent recast layers. Spatters and cracks were absent. ANOVA allowed selecting the significant process parameters and their interactions. ANOVA analysis and ANN models efficiently supported both the investigation and optimization the process.

Yb:KGW laser for hole drilling demonstrated great potentiality in avoiding the defects of the laser-drilling process.

Having great potentiality in eradicating the defects inherent in laser-drilled holes, Yb:KGW laser for hole drilling is expected to become a versatile tool finding broader applications in aerospace and aircraft industries.

Acknowledgements

This work was partially supported by Italian Ministry of Research - MIUR Ministero dell'Istruzione, dell'Università e della Ricerca, Project EURO6 PON01_02238.

References

[1] Campanelli, S.L., Casalino, G., Ludovico, A.D., Bonserio, C. An artificial neural network approach for the control of the laser milling process. International Journal of Advanced Manufacturing Technology, 66, 9-12, 2013, 1777-1784.

[2] Leone, C., Genna, S., Tagliaferri, F., Palumbo, B., Dix, M. Experimental investigation on laser milling of aluminium oxide using a 30 W Q-switched Yb:YAG fiber laser. Optics and Laser Technology 2016, 76, 127-137.

[3] Velotti, C, Astarita, A., Leone, C., Genna, S., Minutolo, F.M.C., Squillace, A. Laser Marking of Titanium Coating for Aerospace Applications. Procedia CIRP 2016, 41, 975-980.

[4] Campanelli, S.L., Casalino, G., Contuzzi, N. Multi-objective optimization of laser milling of 5754 aluminum alloy. Optics and Laser Technology. 52, 2013, 48-56.

[5] Muneer K. M., Al-Ahmari A., Usama U. Multiobjective optimization of Nd:YAG direct laser writing of microchannels for microfluidic applications. Int J Adv Manuf Technology 2015, 81(5), 1363–1377.

[6] Kyoung H. H., Se Won L., Janggil K., Won Y. J. and Chong N. C. Fabrication of a micro-hole array on metal foil by nanosecond pulsed laser beam machining using a cover plate. Journal of Micromechanics and Microengineering 2015, 25.

[7] Wolynskia A., Herrmanna T., Muchab P., Halouic H., L'huilliera J. Laser ablation of CFRP using picosecond laser pulses at different wavelengths from UV to IR. Physics Procedia 2011, 12, 292–301.

[8] Kamlage G., Bauer T., Ostendorf A., Chichkov B. N.. Deep drilling of metals by femtosecond laser pulses. Appl. Phys. A 2003, 77, 307-310.

[7] Weck A., Crawford T.H.R., Wilkinson D.S., Haugen H.K., Preston J.S.. Laser drilling of high aspect ratio holes in copper with femtosecond, picosecond and nanosecond pulses. Appl. Phys. A 2008, 90, 537-543.

[10] Feng Q., Picard Y. N., Liu H., Yalisove S. M., Mourou G. and Pollock T. M.. Femtosecond laser micromachining of single-crystal superalloy. Scripta Materialia 2005, 53, 511-516.

[11] Corcoran A., Sexton L., Seamen B., Ryan P., Byrne G.. The laser drilling of multi-layer aerospace material systems. Journal of Materials Processing Technology 2002, 123, 110-106.

[12] Tyson N. Kim, Kyle Campbell, Alex Groisman, David Kleinfeld, and Chris B. Schaffer. Femtosecond laser-drilled capillary integrated into a microfluidic device. Applied Physics Letters 2005, 86.

[13] Huang H., Lih-Mei Y., Jian L. Micro-hole drilling and cutting using femtosecond fiber laser. Optical Engineering 2014, 53(5).

[14] Ostendorf A., Kamlage G., Chichkov B. N. Precise deep drilling of metals by femtosecond laser pulses. RIKEN Review No. 50 (2003): Focused on Laser Precision Microfabrication (LPM 2002).

[15] Röser F., Eidam T., Rothhardt J., Schmidt O., Schimpf D. N., Limpert J., Tünnermann A. "Millijoule Pulse Energy High Repetition Rate Femtosecond Fiber CPA System," Optics Letters 2007, 32.

[16] Ancona, A., Röser, F., Rademaker, K., Limpert, J., Nolte, S., Tünnermann, A. High speed laser drilling of metals using a high repetition rate, high average power ultrafast fiber CPA system. Optics Express 2008, 16(12).

[17] Qinxin W., Sizuo L., Zhou C., Hongxia Q., Jiannan D., Zhan H. Drilling of aluminum and copper films with femtosecond double-pulse laser. Optics &Laser Technology 80(2016), 116-124

[18] Leitza K., Redlingshöfer B., Reg Y., Ottoa A., Schmidt M.. Metal Ablation with Short and Ultrashort Laser Pulses. Physics Procedia 2011, 12, 230-238.

[19] Rajesh P., Nagaraju U., Harinath G., Vishnu Vardhan T.. Experimental and parametric studies of Nd:YAG laser drilling on austenitic stainless steel. Int J Adv Man. Technol, DOI 10.1007/s00170-015-7639-4.

[20] Douglas C. Montgomery. Design and Analysis of Experiments. 8th Edition, John Wiley & Sons Inc (2012).

[21] Biswas R., Kuar A.S., Mitra S.. Multi-objective optimization of hole characteristics during pulsed Nd:YAG laser microdrilling of gamma-titanium aluminide alloy sheet. Optics and Lasers in Engineering. 2014, 60, 1-11.

[22] Ghoreishi M., Nakhjavani O.B.. Optimisation of effective factors in geometrical specifications of laser percussion drilled holes. Journal of materials processing technology 2008, 196, 303-310.

[23] Priyadarshini M., Pattnaik S.K., Mishra D., Panda S., Dhalmahapatra K.. Multi Characteristics Optimization of Laser Drilling Process Parameter Using Grey Fuzzy Reasoning Method. Materials Today: Proceedings 2015, 1518-1532.

[24] Cheng J., Liu Chang-sheng , Shuo Shang, Dun Liu, Perrie W., Dearden G., Watkins K., 2013 - A review of ultrafast laser materials micromachining. Optics & Laser Technology 46, pp.88–102.

[25] Casalino, G., Ludovico A. Parameter selection by an artificial neural network for a laser bending process. Proceedings of the Institution of Mechanical Engineers, Part B: Journal of Engineering Manufacture, 216, 11, 2002, 1517-1520.

[26] Casalino, G., Facchini, F., Mortello, M., Mummolo, G. ANN modelling to optimize manufacturing processes: the case of laser welding. IFAC-Papers On Line 2016, 49(12), 2016, 378-383.

[27] Zhang H., Jiawena X.. Modeling and Experimental Investigation of Laser Drilling with Jet Electrochemical Machining. Chinese J. of Aeronautics 2010 23(4), 454-460.